

Contending with Space-Time Interaction in the Spatial Prediction of Pollution: Vancouver’s Hourly Ambient PM₁₀ Field

Jim Zidek¹, Li Sun¹ and Nhu Le² Halûk Özkaynak³

¹ University of BC, ² BC Cancer Agency ³ US Environmental Protection Agency

September 27, 2000

Abstract

In this article we describe an approach a way of spatially predicting average hourly concentrations of ambient PM₁₀ in Vancouver. We know our solution also applies to hourly ozone fields and believe it may be quite generally applicable. We use a hierarchical Bayesian approach. At the primary level we model the logarithmic field as a trend model plus Gaussian stochastic residual. That trend model depends on hourly meteorological predictors and is common to all sites. The stochastic component consists of a 24 hour vector response that we model as a multivariate AR(3) temporal process with common spatial parameters. Removing the trend and AR structure leaves “whitened” time series of vector series. With this approach (as opposed to using 24 separate univariate time series models), little loss of spatial correlation in these residuals compared with that in just the detrended residuals (prior to removing the AR component). Moreover our multivariate approach enables predictions for any given hour to “borrow strength” through its correlation with adjoining hours. On this basis we develop an spatial predictive distribution for these residuals at unmonitored sites. By transforming the predicted residuals back to the original data scales we can impute Vancouver’s hourly PM₁₀ field.

KEY WORDS:; space - models; autoregressive processes; spatial interpolation; monitoring networks; spatial correlation.

1 Introduction.

In this article we present a solution to a common problem in the spatial interpolation of short term average levels of space - time fields. We focus our analysis on average hourly concentrations of ambient PM₁₀ in Vancouver. [Interest in particulate air pollution stems from the discovery that elevated levels are associated with acute negative health impacts (*c.f.*).] However we know our solution also applies to hourly ozone fields and believe it may be quite generally applicable.

This paper follows that of Li et al (1999; hereafter LLSZ) who describe the hourly PM₁₀ field over the Greater Vancouver Regional District (GVRD). The authors analyze hourly ambient PM₁₀ concentrations collected in the Vancouver area for the years 1994 to 1996. Data come from 10 (Tapered Element Oscillating Microbalance-TEOM) monitoring stations in the GVRD, different stations starting operation at different times.

The analysis of LLSZ was a prelude to the development of a spatial prediction methodology for imputing unmeasured levels of PM₁₀ at 299 additional locations. However, the intended interpolation methodology, of Le and Zidek (1992) requires of the random field to be interpolated that its realizations: (A) have Gaussian distributions; and (B) be independent. Neither condition holds for our particulate fields. So the data were first logarithmically transformed to insure approximate attainment of (A).

But attaining (B) even approximately proved more challenging. First steps came from the discovery that the temporal pattern of the log-transformed measurements had a remarkable consistency across sites. So a trend model $T(t) = \mu + H(t) + D(t) + L(t) + S(t) + M(t)$ at time t was fitted across all ten monitoring sites, where μ represents the overall mean effect, $H(t)$, the hourly effect, $D(t)$, the day-of-week effect, $L(t)$, the linear trend, $S(t)$, the seasonality effect, and $M(t)$, the meteorological effect. The “detrended residuals” at site x and time t were then computed as $E(x, t) = Y(x, t) - T(t)$ where $Y(x, t)$ denotes the logarithm of the response at site x and time t .

Next, autoregressive and other analyses of the $\{E(x, t)\}$ for each fixed x and varying t led to the adoption of a single AR(3) model for all sites:

$$E(x, t) = \alpha_1 E(x, t - 1) + \alpha_2 E(x, t - 2) + \alpha_3 E(x, t - 3) + e(x, t) \quad (1)$$

where α_1 , α_2 and α_3 are the model coefficients. For fixed x , the $\{e(x, t)\}$ *i.e.* “deAR’d” residuals proved to be quite “white” for the 10 sites, having small auto-correlation.

Spatial prediction would entail imputing the $\{e(x, t)\}$ for 299 sites x not among the original 10 to obtain say $\{\hat{e}(x, t)\}$ for such sites. Next the detrended residuals for those sites would be constructed by taking them to be 0 at times $t = -2, -1$ and using (1) recursively to obtain the \hat{E} 's for those sites. Finally the trend would be added to these imputed residuals to get a series on the original log-PM₁₀ scale.

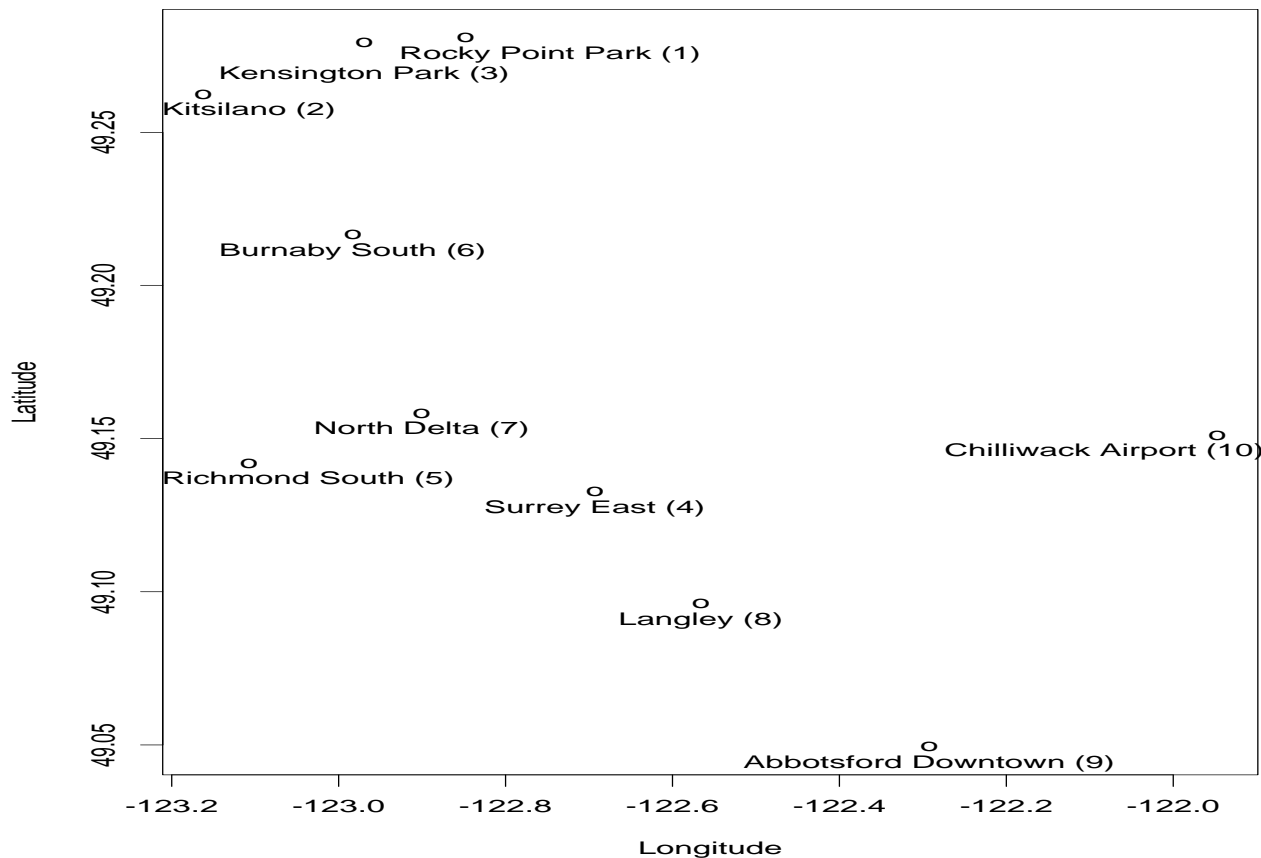


Figure 1. Locations of the 10 PM_{10} Monitoring Stations in Vancouver.

However, subsequent analysis showed that for fixed t and the 10 stations, the deAR'd residuals had not only the expected small autocorrelations but as well they had small between-site cross-correlations (see Table 1). These small correlations contrasted with their substantially larger counterparts for the $\{E(x, t)\}$ (see Table 2) Where had that correlation gone?

Table 1. Cross-correlation $\times 100$ of the deAR'd residuals.

	Site 1	Site 2	Site 3	Site 4	Site 5	Site 6	Site 7	Site 8	Site 9	Site 10
Site 1	100	21	28	26	16	28	23	22	21	16
Site 2	21	100	21	20	28	26	22	17	19	12
Site 3	28	21	100	22	14	27	27	20	14	15
Site 4	26	20	22	100	16	26	30	32	23	17
Site 5	16	28	14	16	100	19	21	16	19	13
Site 6	28	26	27	26	19	100	35	18	18	14
Site 7	23	22	27	30	21	35	100	23	23	15
Site 8	22	17	20	32	16	18	23	100	25	19
Site 9	21	19	14	23	19	18	23	25	100	24
Site 10	16	12	15	17	13	14	15	19	24	100

Table 2. Cross-correlation $\times 100$ of detrended residuals

	Site 1	Site 2	Site 3	Site 4	Site 5	Site 6	Site 7	Site 8	Site 9	Site 10
Site 1	100	41	59	50	33	56	50	44	44	37
Site 2	41	100	40	41	55	50	43	36	39	25
Site 3	59	40	100	50	27	61	54	41	34	34
Site 4	50	41	50	100	35	59	65	62	50	33
Site 5	33	55	27	35	100	36	36	35	39	25
Site 6	56	50	61	59	36	100	65	46	42	33
Site 7	50	43	54	65	36	65	100	52	47	31
Site 8	44	36	41	62	35	46	52	100	50	40
Site 9	44	39	34	50	39	42	47	50	100	46
Site 10	37	25	34	33	25	33	31	40	46	100

In a follow-up analysis the authors of the present paper found that spatial correlation had “leaked” into lag-one hourly cross-correlations between sites. Substantial correlation remains between $\{e(x, t)\}$ and $\{e(x', t - 1)\}$ at any two sites x and x' for varying t .

This finding reveals that the 10 parallel short-term time average series have a complex spatial-temporal structure that cannot be modeled through univariate time-series methods applied one site at a time as can for example that for daily average (Li et al 1999). Moreover, a naive multivariate auto-regressive approach cannot be used to circumvent the problem, as we now explain.

That approach would use the detrended residuals series for all of the 10 sites in the model:

$$\mathbf{E}(t) = \sum_{i=1}^p \mathbf{A}_i \mathbf{E}(t - 1) + \mathbf{e}(t) \tag{2}$$

where the $\{\mathbf{A}_i\}$ are the 10×10 matrices of model coefficients, the $\mathbf{E}(t) = (E(1, t), \dots, E(10, t))'$ for all t and the $\{\mathbf{e}(t)\}$ are the multivariate deAR'd residual vectors.

This approach would block the spatial correlation in the E-series from “leaking” into lag-1 spatial cross-correlation in the e-series. With the resulting, increased cross-correlation in the lag-0 e-series, success in constructing the \hat{e} series for the remaining 299 stations would be assured. To that extent the multivariate method would succeed.

The difficulty arises when we attempt to construct the \hat{E} series. Our 10×10 A coefficient matrices would need to be extended to 299×299 matrices for all the sites. This seems to be an even more challenging problem than the interpolation of the series themselves. We see no way of solving it and need an alternative approach.

The analysis of LLSZ suggests possible alternative approaches. Since the detrended PM10. hourly series was found to have an AR(3) structure, we would expect successive detrended log daily averages to have markedly smaller autocorrelations than their hourly counterparts. Theoretical considerations (see the Appendix) indicate the possible lag 1 cross-correlations should be small as well. Thus the spatial-temporal complexities described above for the hourly series should be circumvented for daily fields. At the same time, for many purposes interpolated daily values should suffice. In particular studies in spatial epidemiology (*cf.*) typically rely on such daily values. These heuristics are confirmed in a companion paper (Li et al 1999).

However for other purposes such as setting regulatory standards or modeling human exposure, hourly values may be needed. One exploratory approach would be to analyze the data for one specified hour at a time. The AR(3) structure of LLSZ suggests that these hourly values will be approximately independent since they are separated by 23 hours. Moreover we can fit different models for each hour. The varying hourly spatial covariance structure will allow us to capture the shifting wind field over the day without explicitly modeling it. That analysis will be further enhanced by fitting different models for the different seasons to allow for seasonal variations in the daily wind field. We present the results of that analysis elsewhere.

The one hour-at-a-time analysis suffers from the disadvantage that we cannot “borrow strength” from the hours adjoining that of interest. Thus a multivariate approach is preferred (reference Le et al paper) and the the last of our approaches tries to improve on the second in this way. As a preliminary step we returned to the second approach to see if we find natural homogeneous clusters of 24 hours. We expected to see one, two or more hour-clusters that might be grouped into natural multivariate response vectors for subsequent analysis. However we found no such clusters. Thus we combined all 24 hours into a single vector-valued time series.

Other approaches to the analysis of short-term pollution field aggregates have been developed. For hourly ozone concentrations, prediction methods are developed by Carroll et al (1997) and Guttorp et al (1994). The former differs

markedly from the latter and that presented here for particulate fields. In particular Carroll and his co-authors assume both spatial and temporal homogeneity for their study based in Houston.

That assumption does simplifies finding a parametric model for space-time covariances. Carroll et al (1997) fit their model and plug these estimates into their prediction formulas. However, the added uncertainty seems not to have been reflected in subsequent analysis. Such uncertainty can be appreciable and adds considerably to the length of say 95% prediction intervals. (*c.f.* Oliviera et al 1997, and Sun 1998). In any event in our approach to finding a spatial prediction strategy, we have sought to incorporate that uncertainty fully (see Le and Zidek 1992, Le, Sun and Zidek 1997 and Le, Sun and Zidek 2000).

As joint discussants for the paper of Carroll et al (1997), Guttorp, Meiring and Sampson (GMS) criticize specifically for Houston, the assumption of temporal homogeneity. Moreover they have difficulty in general with methods for interpolating environmental fields that invoke the assumption of spatial homogeneity. Houston fields notwithstanding GMS like us have found that assumption generally too simplistic.

We believe the methods proposed in this paper overcome some of the difficulties described above. In the next section we describe the underlying space-time model for the PM₁₀ in Vancouver and in particular find a trend model that incorporates not only structural time trends but meteorology as well. We go on to find a single ("all-site") 24 dimensional autoregressive model that describes the residuals obtained by removing the trend. In Section 3 we very briefly describe the spatial interpolation procedures we use in this paper. In particular we describe there, the Sampson-Guttorp approach (Sampson and Guttorp 1992, Guttorp, and Sampson 1994) to estimating the spatial covariance we need to implement the procedure. In that section we also present our multivariate predictors. Concluding remarks are found in Section 4.

2 The Trend and Autoregressive Model Components.

In this section we develop a trend model for Vancouver's hourly log PM₁₀ field. It includes both structural time trends as well as meteorological predictors. As well we find a multivariate autoregressive model to describe the stochastic component of the all-sites model

2.1 The Trend Model.

We consider hourly measurements of meteorological variables at the Vancouver Airport, 1996:

Table 3. Descriptive Statistics For The Meteorological Predictors.

Variable	Unit	N	Mean	Std Dev	Minimum	Maximum
Visibility	km	8775	33.59	14.67	0.20	64.40
Pressure	kilopascals	8773	101.60	0.84	97.94	104.14
Relative Humidity	%	8773	73.48	13.40	16.00	100.00
Dew Point	deg C	8773	4.96	5.98	-19.80	16.50
Temperature	deg C	8773	9.75	6.58	-11.70	27.40
Wind in North	km/hr	8775	-1.36	7.52	-38.41	33.42
Wind in East	km/hr	8775	2.12	12.12	-55.44	43.00
Rain	0 or 1	8784	0.11	0.31	0	1.00

Physical considerations led the investigators to exclude "Dew Point Temperature" at the outset. We believed it to be related to the product of "Temperature" and "Relative Humidity". Moreover the need to avoided collinearity puts a premium on parsimonious models.

Likewise physical considerations suggested that "Visibility", "Pressure" and "Relative Humidity" be incorporated as predictors through their logarithms. However, "Relative Humidity" was first replaced by 1-"Relative Humidity" (truncated below at 0.05) so that the resulting variable is expected to have a positive association with hourly log PM₁₀.

To reduce collinearity among the variables included in the models (and their interactions), all variables except "Rain" were centered by the subtraction of their sample averages. To make the size of their model coefficients more comparable, the centered variables were divided by their sample standard deviations. [The very large number of observations in the time series makes the standard errors of the latter negligible.]

In the end the following variables were used in building a meteorological trend model:

- LVIZ = $[\log(Visibility) - \overline{\log(Visibility)}] / SD(\log(Visibility))$;

- $LPRS = [\log(Pressure) - \overline{\log(Pressure)}] / SD(\log(Pressure));$
- $LRH = [\log(100 - Relative.Humidity) - \overline{\log(100 - Relative.Humidity)}] / SD(\log(100 - Relative.Humidity));$
- $TEM = (Temperature - \overline{Temperature}) / SD(Temperature);$
- $WDX = (Wind.in.North - \overline{Wind.in.North}) / SD(Wind.in.North);$
- $WDY = (Wind.in.East - \overline{Wind.in.East}) / SD(Wind.in.East).$

Regressing log PM₁₀ on these variables and their interactions (up to order two) in a preliminary analysis that avoided excessive complexity by ignoring temporal trends, we found that the BIC criterion included all the variables as main effects in the model plus the following interactions:

LVIZ*LPRS; LVIZ*TEM; LVIZ*WDX; LVIZ*RAIN; LPRS*TEM; LPRS*WDX; LPRS*RAIN;LRH*TEM;
 LRH*WDY; TEM*TEM; TEM*WDX; TEM*WDY; WDX*WDX; WDX*WDY; WDY*WDY.

These selected meteorological components were then incorporated into the full trend model as described in the introduction. Thus we added: HOUR; DAY; LIN (linear trend); COS1 and SIN1 (annual seasonal cycles); COS2 and SIN2 (semi-annual cycles); COS3 and SIN3 (monthly cycles). The analysis of the overall model fit is given in Table 4.

Table 4. Overall Analysis of log PM₁₀ Model Fit.

Source	DF	Sum of Squares	Mean Square	F Value	Pr > F
Model	58	9582	165.21	615.16	0.0001
Error	85170	22874	0.26856		
Corrected Total	85228	32456			
	R-Square	C.V.	Root MSE	log(PM ₁₀) Mean	
	0.295	20.68	0.51823	2.50540	

We show the decomposition of variation by individual components in Appendix B. Also given in the Appendix B are the estimated coefficients, their t-values and standard errors of the fitted model.

Figure 2 displays the temporal components in the trend model, that is, the hourly effect, day-off-week effect and the seasonalities with the added linear trend.

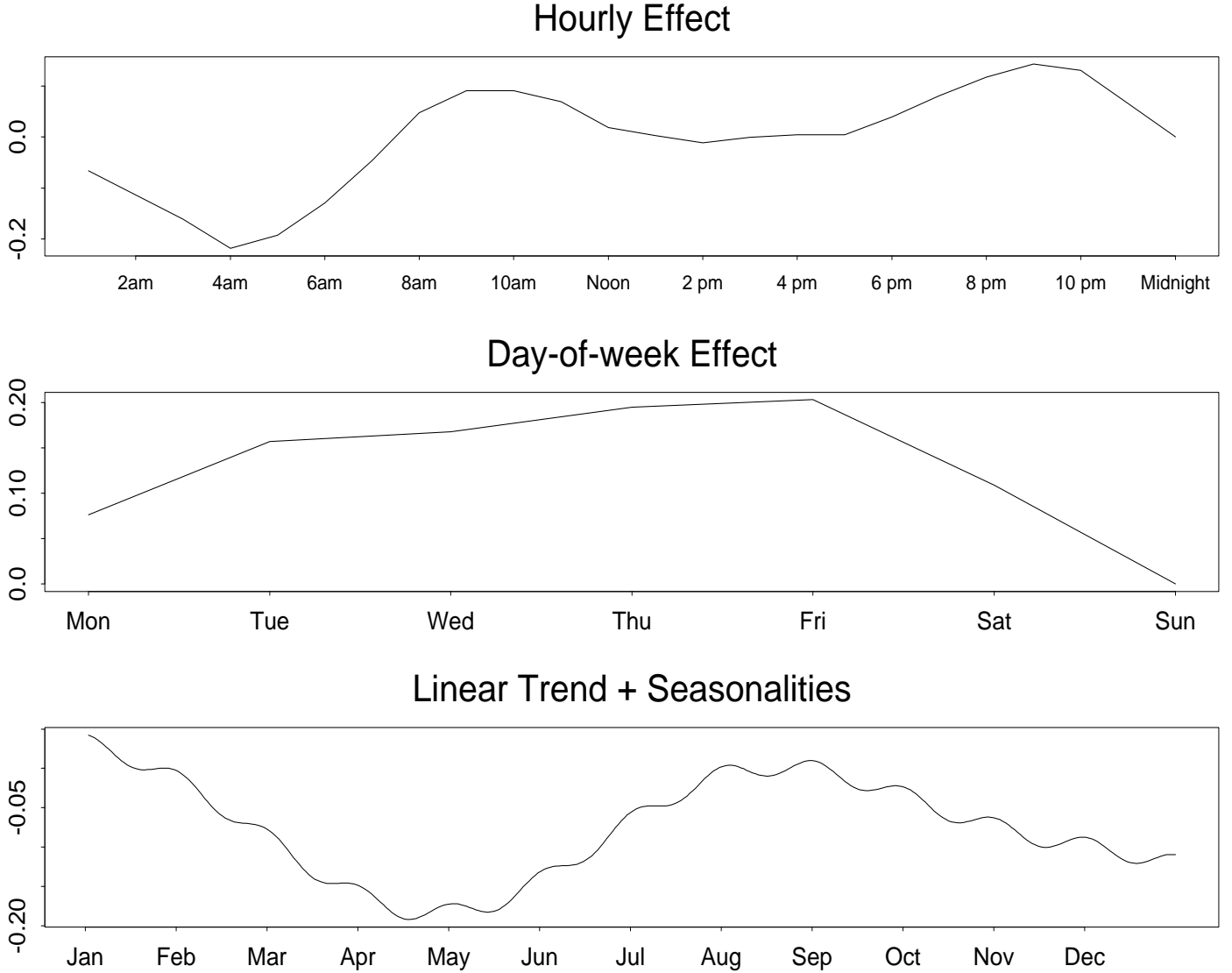


Figure 2. Fitted Hourly, Day-of-week Effects and Seasonalities in the $\log PM_{10}$ Model.

2.2 The Multivariate Autoregressive Model Component.

Let $W(x, d)$ denote the 24 dimensional detrended residual vector at site x , on day d . The AIC criterion selects an order three auto-regression model

$$W(x, d) = M_1 W(x, d - 1) + M_2 W(x, d - 2) + M_3 W(x, d - 3) + \epsilon(x, d), \quad (3)$$

for $d = 1, \dots, 360$. Coefficients are estimated using the method of Burg (1967). The estimated coefficient M matrices are given in the Appendix. The deAR'd residuals resulting from the multivariate autoregressive process are then computed by

$$X(x, d) = W(x, d) - \hat{M}_1 W(x, d - 1) - \hat{M}_2 W(x, d - 2) - \hat{M}_3 W(x, d - 3). \quad (4)$$

With the trend and autoregressive components estimated, we may now find the deAR'd residuals by subtracting both of these components from the original log transformed series of PM_{10} concentrations. Before leaving this section we need to show that little spatial correlation has been lost (“leaked”) in the process; otherwise our approach will have failed.

To this end we computed the empirical spatial correlation matrix after the multivariate AR fit, namely the correlation matrix of the deAR'd residuals. They may be seen in Table 5 and must be compared with those in Table 1 for the detrended but not deAR'd series.

Table 5. Correlation $\times 100$ After Removing the Multivariate AR Effect.

	Site 1	Site 2	Site 3	Site 4	Site 5	Site 6	Site 7	Site 8	Site 9	Site 10
Site 1	100	33	51	41	25	46	39	35	34	31
Site 2	33	100	36	32	44	40	33	27	30	20
Site 3	51	36	100	41	22	51	43	33	24	26
Site 4	41	32	41	100	26	49	54	54	41	30
Site 5	25	44	22	26	100	29	29	26	31	19
Site 6	46	40	51	49	29	100	55	37	33	27
Site 7	39	33	43	54	29	55	100	43	37	26
Site 8	35	27	33	54	26	37	43	100	42	36
Site 9	34	30	24	41	31	33	37	42	100	40
Site 10	31	20	26	30	19	27	26	36	40	100

That comparison reveals that little spatial correlation has been removed by removing the temporal correlation to whiten the residuals. Thus, we are prepared for the next step in our analysis, that of constructing a predictive distribution for interpolating the field.

3 Interpolating the Hourly PM_{10} Field.

As the first step in constructing our spatial predictive distribution, the primary objective of this section, we must estimate the spatial covariance field. We do that in the next section using a method developed by Sampson and Guttorp (the SG method; Guttorp and Sampson 1994; Sampson and Guttorp 1992).

We do not give here a complete description of the methodology that has been published elsewhere (Brown et al 1994; Sun et al 1997). For brevity we give just the elements needed in the construction.

3.1 GIW model with Kronecker structure

Let $X(d)$ be the 240-dimensional vector formed from the deAR'd residual vectors $X(x, d)$ at the 10 sites. The work described in LLSZ suggests that we reasonably approximate the distribution of the the deAR'd hourly log PM_{10} field by a multivariate Gaussian distribution. Thus given the spatial covariance matrix Σ at any particular time (assumed to be constant over time) we adopt the following Gaussian- Inverted-Wishart (GIW) model for the deAR'd residuals $X(d)$:

$$X(d) | \Sigma \sim N(0, \Sigma), \quad d = 1, \dots, 366, \tag{5}$$

$$\Sigma | \Psi \sim IW(\Psi, \delta^*)$$

where

$$\Psi = \Lambda \otimes \Omega, \quad \text{with } \Lambda : 10 \times 10, \text{ and } \Omega : 24 \times 24. \tag{6}$$

Here Λ represents the spatial covariance between the 10 monitoring sites, Ω that between hours.

It can be shown (*cf.* Brown et al 1994) that the marginal distribution of $X(d)$ is

$$X(d) \sim t_{240}(0, \delta^{-1}\Lambda \otimes \Omega, \delta), \tag{7}$$

where $\delta = \delta^* - 240 + 1$.

The method of moments developed by (Kibria et al 2000) is used to estimate the model parameters. The estimate of the degrees of freedom is $\hat{\delta}^* = 298.6$ or the estimated of δ is $\hat{\delta} = 298.6 - 240 + 1 = 59.6$. The estimates of Λ and Ω are provided in the Appendix D.

The spatial correlation matrix obtained from the estimate of Λ is shown in Table 6.

Table 6. Correlation $\times 100$ Between Sites Obtained from Fitting a Kronecker Product Covariance.

	Site 1	Site 2	Site 3	Site 4	Site 5	Site 6	Site 7	Site 8	Site 9	Site 10
Site 1	100	46	67	55	37	63	54	48	48	45
Site 2	46	100	48	42	58	52	41	36	43	28
Site 3	67	48	100	59	29	70	59	50	36	38
Site 4	55	42	59	100	34	68	73	72	56	41
Site 5	37	58	29	34	100	38	35	34	43	26
Site 6	63	52	70	68	38	100	71	56	48	41
Site 7	54	41	59	73	35	71	100	61	49	36
Site 8	48	36	50	72	34	56	61	100	56	49
Site 9	48	43	36	56	43	48	49	56	100	53
Site 10	45	28	38	41	26	41	36	49	53	100

The corresponding correlation between hours using the estimate of Ω is given in Table 7.

Table 7. Correlations $\times 100$ Between Times Obtained from Fitting a Kronecker Product Covariance.

-	64	54	49	42	34	22	14	10	9	13	13	8	9	7	3	-5	-4	-1	0	6	6	4	2
64	-	71	57	51	41	29	15	11	10	13	14	9	11	12	4	-0	1	2	3	6	7	6	9
54	71	-	77	67	56	41	28	20	19	20	18	12	9	10	6	1	4	-1	-2	2	2	1	6
49	57	77	-	78	66	52	39	31	26	25	22	16	11	9	9	0	2	0	-3	2	3	1	5
42	51	67	78	-	82	66	53	42	37	33	25	19	15	10	11	6	7	3	-0	4	4	2	6
34	41	56	66	82	-	79	60	48	41	37	32	22	16	11	8	4	3	1	-2	4	5	3	7
22	29	41	52	66	79	-	74	58	44	37	32	24	20	13	12	10	9	10	9	12	11	9	10
14	15	28	39	53	60	74	-	77	57	48	37	31	27	22	22	16	16	16	15	15	17	13	13
10	11	20	31	42	48	58	77	-	76	64	49	40	31	26	27	22	22	21	17	17	19	16	18
9	10	19	26	37	41	44	57	76	-	79	63	50	37	31	32	28	28	25	22	17	20	16	19
13	13	20	25	33	37	37	48	64	79	-	80	67	52	41	39	36	31	25	21	19	23	18	22
13	14	18	22	25	32	32	37	49	63	80	-	78	61	51	43	40	35	30	27	27	29	24	27
8	9	12	16	19	22	24	31	40	50	67	78	-	80	66	56	51	46	36	34	31	32	27	28
9	11	9	11	15	16	20	27	31	37	52	61	80	-	79	66	62	53	43	40	34	34	29	29
7	12	10	9	10	11	13	22	26	31	41	51	66	79	-	78	70	61	49	43	39	39	34	36
3	4	6	9	11	8	12	22	27	32	39	43	56	66	78	-	80	67	53	47	41	39	36	35
-5	-0	1	0	6	4	10	16	22	28	36	40	51	62	70	80	-	82	67	59	49	46	43	39
-4	1	4	2	7	3	9	16	22	28	31	35	46	53	61	67	82	-	80	68	56	52	46	42
-1	2	-1	0	3	1	10	16	21	25	25	30	36	43	49	53	67	80	-	81	69	64	56	53
0	3	-2	-3	-0	-2	9	15	17	22	21	27	34	40	43	47	59	68	81	-	83	72	67	61
6	6	2	2	4	4	12	15	17	17	19	27	31	34	39	41	49	56	69	83	-	86	76	70
6	7	2	3	4	5	11	17	19	20	23	29	32	34	39	39	46	52	64	72	86	-	87	80
4	6	1	1	2	3	9	13	16	16	18	24	27	29	34	36	43	46	56	67	76	87	-	88
2	9	6	5	6	7	10	13	18	19	22	27	28	29	36	35	39	42	53	61	70	80	88	-

3.2 SG Algorithm and Spatial Prediction.

The estimated spatial covariance matrix from the Gaussian Inverted Wishart model obtained in the last subsection together with the latitude and longitude of the ten sites must now be input to the Sampson-Guttorp algorithm. That algorithm extends the covariance matrix obtained for just the 10 monitoring sites to one for the 299 census tracts plus the 10 existing monitoring sites in Great Vancouver. Denote the extended Lambda matrix by $\Lambda^{[u,g]}$. Let

$$X_d^{[u,g]} = \begin{pmatrix} X_d^{[u]} \\ X_d^{[g]} \end{pmatrix}$$

be the 309×24 response residual matrix on day d , where $X_d^{[u]}$ is a 299×24 matrix with its i -th row being the 24 hour response vector at census tract i . Similarly $X_d^{[g]}$ is a 10×24 matrix, its i -th row being the 24 observed residual values at station i on day-hour d . Then it is shown (Brown et al 1994) that $X_d^{[u,g]}$ has a matrix-t distribution, namely

$$X_d^{[u,g]} \sim t_{309 \times 24}(0, \delta^{-1} \Lambda^{[u,g]} \otimes \Omega, \delta).$$

Moreover, the conditional distribution of $(X_d^{[u]}|X_d^{[g]})$ is given by

$$(X_d^{[u]}|X_d^{[g]}) \sim t_{299 \times 10}(\mu_d^*, (\delta + 10)^{-1} \Lambda^* \otimes \Omega_d^*, \delta + 10)$$

where

$$\mu_d^* = \Lambda_{12} \Lambda_{22}^{-1} X_d^{[g]}, \quad \Lambda^* = \Lambda_{11} - \Lambda_{12} \Lambda_{22}^{-1} \Lambda_{21}, \quad \Omega_d^* = \Omega + \frac{1}{\delta} X_d^{[g]} \Lambda_{22}^{-1} X_d^{[g]}.$$

A central idea underlying the SG method is that of transforming the geographic plane (G-space) on which the census tracts are situated into a "dispersion" plane (D-space) in such a way that inter-site correlations become monotonic functions of the dispersion plane distances between them. The extended spatial covariance can be constructed then by fitting one of the standard spatial covariance (or equivalently "dispersion") models to the empirical covariances estimated for the original 10 sites.

The result of applying that algorithm The SG algorithm is visually illustrated in the figure below.

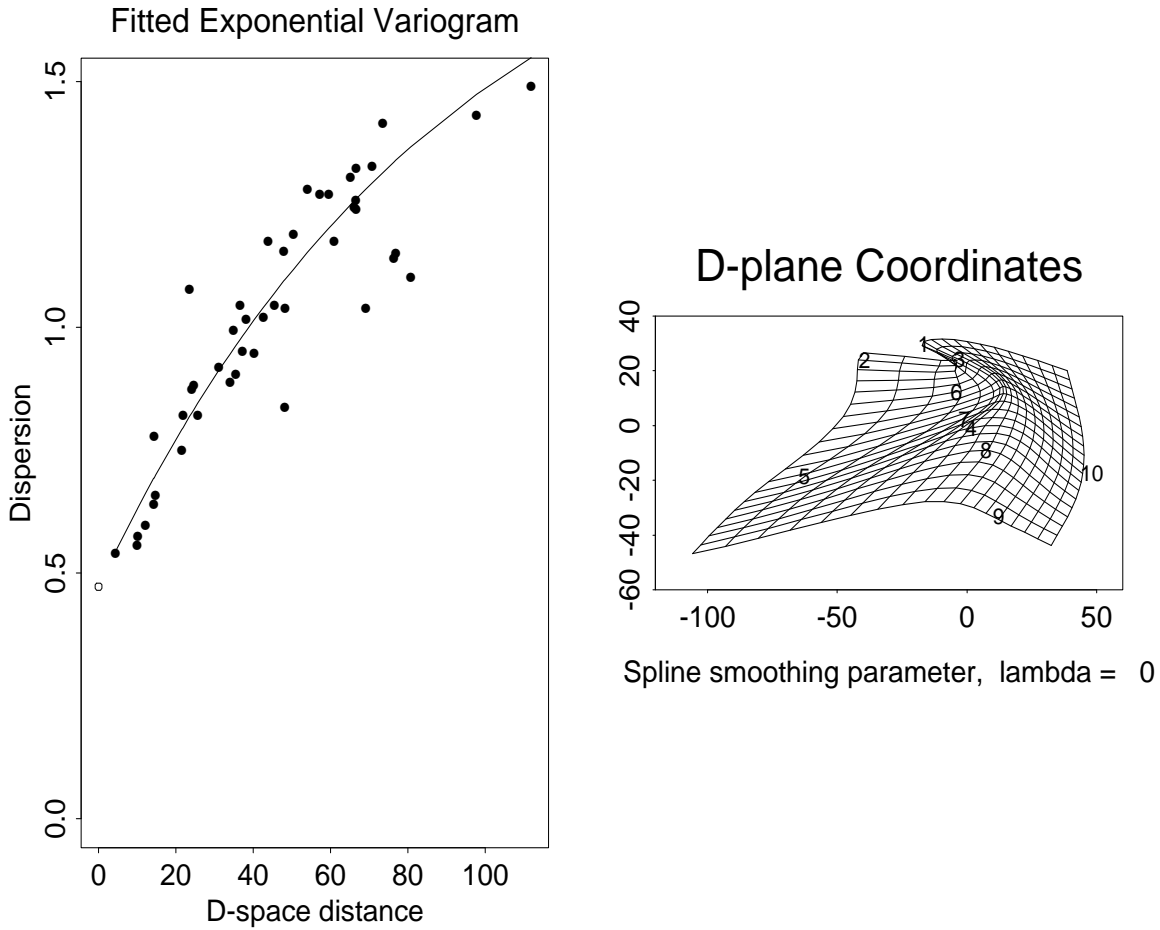


Figure 3. Dispersion Transformation in The SG Algorithm.

The left panel in that figure displays the fitted dispersion function as an exponential form. From the second panel, we find that to reach D-space isotropy, Site 5 (Richmond) has to be pushed out from the group of other sites, while Site 9 (Abbotsford) and Site 10 (Chilliwack) have to be moved into the center of region. Meanwhile, Site 1 (Rocky Point Park) and Site 3 (Kensington Park) need to move toward to the West and Site 2 (Kitsilano) need to move to the East.

After obtaining the required estimate of the spatial covariance, we are able to construct the spatial predictive distribution. Its mean can be used to 'interpolate' the hourly PM field. Initially this is done with the deAR'd residual field. The interpolated hourly log PM₁₀ fields are obtained by first adding the AR component of Section 2.2, and then adding the trend component of Section 2.1 to the interpolated residuals. This completes the construction of the spatial predictor. Figure 4 shows the PM₁₀ fields in the morning on a summer day (Wednesday, August 7, 1996).

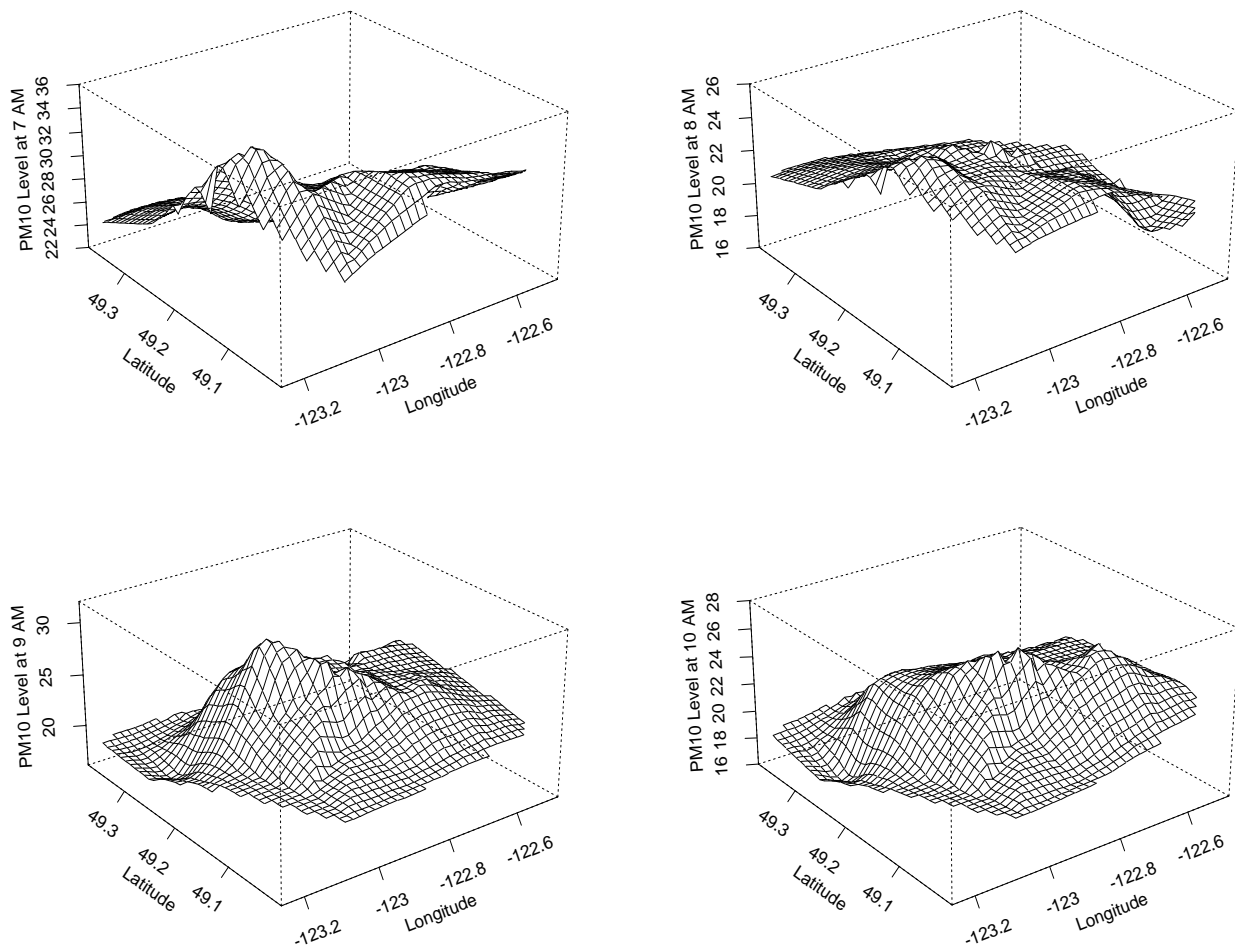


Figure 4. Interpolated PM_{10} Fields in The Morning, Wednesday, August 7, 1996.

The surface has a peak in Richmond at 7AM (we notice this is typical in the summer mornings), while the concentration level reaches its maximum in the downtown area at 9AM. The surface is relatively flat at 10AM .

4 Concluding Remarks.

In this paper we have shown that a multivariate spatial predictor can be used to overcome the problem of space-time interaction for the PM_{10} short term average pollution. The 24 consecutive hourly concentrations at each site are treated as a multivariate response vector for that purpose.

The method does not require that an hourly AR model be specified. Instead the daily response vectors are modeling as a multivariate (AR(3)) process. We thereby avoid the risk of misspecifying the hour-by-hour stochastic structure. But more fundamentally, we avoid spatial correlation leakage shown in this paper to occur when the latter is attempted.

This approach is demonstrated with Vancouver's log PM_{10} field. We see there quite a lot of hour-to-hour variation. At the same time our multivariate approach assures coherence between the interpolated fields for success hours. Moreover, it makes the successive spatial hourly predictions more accurate through the borrowing of strength from adjacent hours.

The method's capability to borrow strength is being enhanced through an extension to the case of multi-pollutant fields. Then strength will come not only from adjacent hours but from pollutants correlated with that of central interest. A description of that method will be published elsewhere.

5 Disclaimer.

The U.S. Environmental Protection Agency through its Office of Research and Development partially funded the research described here under a Cooperative Agreement # CR825267-01 to Harvard University School of Public Health. It has been subjected to Agency review and approved for publication. Mention of trade names or commercial products does not constitute an endorsement or recommendation for use.

References

- [1] Bates, DV, Baker-Anderson, M and Sizto, R (1990). Asthma attack periodicity: a study of hospital emergency visits in Vancouver. *Environmental Research*, 51, 51-70.
- [2] Brown, PJ, Le, ND and Zidek, JV (1994). Multivariate spatial interpolation and exposure to air pollutants. *Canadian Journal of Statistics*, 22, 489-509.
- [3] Burg, JP (1972). The relationship between maximum entropy spectra and maximum likelihood spectra. *Geophysics*, 37, 375-376.
- [4] Burnett, RT, Dales, R, Krewski, D, Vincent, R, Dann, T and Brook, JR (1995). Associations between ambient particulates sulfate and admissions to Ontario hospitals for cardiac and respiratory diseases. *Amer. Jour. Epidemiology*, 142, 15-22.
- [5] Carroll, RJ, Chen, R, George, EI, Li, TH, Newton, HJ, Schmiediche, H and Wang, N (1997). 'Ozone exposure and population density in Harris County, Texas'. *Journal of the American Statistical Association*, 92, 392-415.
- [6] De Oliveira, V., Kedem, B. and Short, D.A. (1997). "Bayesian Prediction of Transformed Gaussian Random Fields." *J Amer. Statist. Assoc.* 92, 1422-1433.
- [7] Dockery, DW, Schwartz, J and Spengler, JD (1992). Air pollution and daily mortality: associations with particulates and acid aerosols. *Environmental Research*, 59, 362-373.
- [8] Guttorp, P and Sampson, PD (1994). Methods for estimating heterogeneous spatial covariance functions with environmental applications in Handbook of Statistics VII Environmental Statistics. Eds. GP Patil and CR Rao, New York: North-Holland/Elsevier, pp. 663-690.
- [9] Li, K, Le, ND, Sun, L and Zidek, JV (1999). Spatial-temporal Models for ambient hourly PM₁₀ in Vancouver. *Environmetrics*, 10, 321-338.
- [10] Le, ND and Zidek, JV (1992). Interpolation with Uncertain Spatial Covariance: a Bayesian Alternative to Kriging. *Journal Multivariate Analysis.*, 43, 351-374.
- [11] Le, ND, Sun, L and Zidek, JV (2000). Bayesian spatial interpolation and backcasting using the Gaussian inverted Wishart model. Submitted.
- [12] Pope, CA, Thun, MJ, Namboodiri, MM, Dockery, DW, Evans, JS, Speizer, FE and Heath, CW (1995). Particulate air pollution as a predictor of mortality in a prospective study of U.S. adults. *Amer. Jour. Respiratory and Critical Care Medicine*, 151, 669-674.
- [13] Ostro, BD, Lipsett, MJ, Wiener, MB and Selner, JC (1991). Asthmatic responses to airborne acid aerosols. *Jour. Public Health*, 81, 694-702.
- [14] Reomer, W, Hoek, G and Brunekreef, B (1993). Effect of ambient winter air pollution on respiratory health of children with chronic respiratory symptoms. *Amer. Review of Respiratory Diseases*, 147, 118-124.
- [15] Sampson, P and Guttorp, P (1992). "Nonparametric estimation of nonstationary spatial covariance structure." *J. Amer. Statist. Assoc.* Vol.87 No. 417, 108-119.
- [16] Schwartz, J, Slater, D, Larson, TV, Pierson, WE, Koenig, JQ (1993). Particulate air pollution and hospital emergency visits for asthma in Seattle. *Amer. Review of Respiratory Diseases*, 147, 826-831.
- [17] Sun, W.(1998). "Comparison of a CoKriging Method With a Bayesian Alternative". *Environmetrics*, 9, 445-457.

- [18] Sun, W, Le, ND, Zidek, JV and Burnett, RT (1998) Assessment of a Bayesian multivariate spatial interpolation approach for health impact studies. *Environmetrics*, 9, 565-586.
- [19] Le, ND, Sun, W and Zidek, JV (1997). Bayesian multivariate spatial interpolation with data missing by design, *J.R.Statist.Soc.B* 59,5-1-510.

A Cross-correlation Leakage.

Consider AR(1) process for site x :

$$E(x, t) = \alpha E(x, t - 1) + e(x, t).$$

It can be shown that

$$\begin{aligned} \text{cor}[E(x, t), E(x', t)] &= \text{cor}[e(x, t), e(x', t)] \\ &+ \frac{\alpha}{\sqrt{1 - \alpha^2}} (\text{cor}[E(x, t - 1), e(x', t)] + \text{cor}[E(x', t - 1), e(x, t)]). \end{aligned}$$

If the lag-one cross correlation $\text{cor}[E(x, t - 1), e(x', t)] = 0$ for any sites x and x' (this is true for a multivariate AR process), then

$$\text{cor}[E(x, t), E(x', t)] = \text{cor}[e(x, t), e(x', t)],$$

that is, the spatial correlations of the detrended residuals are the same as spatial correlations of the deAR'd residuals.

When the lag-one cross correlation $\text{cor}[E(x, t - 1), e(x', t)]$ numerically not zero, the correlation leakage occurs. This is exactly what happens with the hourly log PM10 residuals.

The following table shows the lag one cross-correlation leakage with the hourly data.

Table 8. Lag-one cross correlation $\times 100$

	Site 1	Site 2	Site 3	Site 4	Site 5	Site 6	Site 7	Site 8	Site 9	Site 10
Site 1	-5	6	8	7	5	6	7	8	9	12
Site 2	8	-0	9	10	9	11	9	6	7	6
Site 3	14	6	0	13	3	11	11	11	10	12
Site 4	10	7	9	-0	6	11	11	10	11	10
Site 5	7	14	7	10	3	11	7	6	9	5
Site 6	13	8	15	14	3	-2	12	11	10	10
Site 7	12	8	10	17	6	12	1	13	12	9
Site 8	6	6	4	12	8	8	8	-7	10	10
Site 9	7	8	5	9	7	8	7	7	-3	11
Site 10	5	5	5	5	6	6	5	6	9	5

It is also noticed when $\text{cor}[E(x, t - 1), e(x', t)]$ is fixed, the bigger temporal correlation (i.e., the bigger α) the bigger leakage of the spatial correlation. If we fit an AR(1) model with the hourly log PM10 detrended residual, the estimated coefficient of α will be 0.77; this confirms the drop of the correlations through the AR modeling.

On the contrary, we also find there is no spatial correlation leakage with the log PM10 daily data which are obtained as the measurements of the daily average.

B The Trend Model in Detail.

We show the decomposition of variation by individual components in the following table. All component sums of squares in the Table gave a p-value of much less than 0.01 (in fact 0.0001) except for COS1 (0.06) and SIN3 (0.59). [These high levels of significance are in part an artifact of the very large number of observations in the series.] However these two insignificant components were retained for symmetry with their periodic partners.

Table 5. Partial Sum of Squares By Individual Components.

Source	DF	Type III SS	Mean Square	F Value
HOUR	23	736.11	32.00	119.17
DAY	6	372.31	62.05	231.05
LIN	1	31.24	31.24	116.34
COS1	1	0.93	0.93	3.48
SIN1	1	90.01	90.01	335.17
COS2	1	12.01	12.01	44.74
SIN2	1	20.73	20.73	77.19
COS3	1	4.91	4.91	18.29
SIN3	1	0.08	0.08	0.28
LVIZ	1	184.41	184.41	686.67
LPRS	1	207.86	207.86	773.96
LRH	1	7.90	7.90	29.40
TEM	1	92.46	92.46	344.28
WDX	1	133.32	133.32	496.43
WDY	1	93.61	93.61	348.56
RAIN	1	20.12	20.12	74.92
LVIZ*LPRS	1	17.08	17.08	63.59
LVIZ*TEM	1	69.31	69.31	258.09
LVIZ*WDX	1	33.60	33.60	125.13
LVIZ*RAIN	1	25.52	25.52	95.03
LPRS*TEM	1	108.44	108.44	403.76
LPRS*WDX	1	8.32	8.32	30.97
LPRS*RAIN	1	17.36	17.36	64.65
LRH*TEM	1	27.77	27.77	103.42
LRH*WDY	1	41.77	41.77	155.52
TEM*TEM	1	197.61	197.61	735.79
TEM*WDX	1	46.46	46.46	172.99
TEM*WDY	1	69.96	69.96	260.48
WDX*WDX	1	50.74	50.74	188.94
WDX*WDY	1	49.12	49.12	182.88
WDY*WDY	1	470.96	470.96	1753.63

The following table presents the estimated coefficients, their t-values and standard errors of the fitted model, all in the units of of log PM₁₀, namely log μgm^{-3} . All the p-values are less than 0.01 (in fact 0.0001) except for HOURS 12 (0.14), 13 (0.82), 14 (0.39), 15 (0.95), 16 (0.75), as well as 17 (0.73), for COS1 (0.06) and SIN3 (0.59).

Table 9. Coefficients of The Fitted Model and Associated Standard Errors and T Values.

Parameter	1000× Coefficient Estimate	T-value	1000× Standard Error
INTERCEPT	2427.7	159.74	15.2
HOUR 1	-661.7	-5.38	12.3
HOUR 2	-113.7	-9.23	12.3
HOUR 3	-160.8	-13.04	12.3
HOUR 4	-218.1	-17.65	12.4
HOUR 5	-192.5	-15.56	12.4
HOUR 6	-129.4	-10.47	12.4
HOUR 7	-46.4	-3.76	12.3
HOUR 8	47.8	3.88	12.3
HOUR 9	91.0	7.37	12.3
HOUR 10	90.4	7.29	12.4
HOUR 11	68.8	5.52	12.5
HOUR 12	18.4	1.47	12.6
HOUR 13	2.9	0.23	12.7
HOUR 14	-11.0	-0.87	12.7
HOUR 15	-0.8	-0.06	12.7
HOUR 16	4.1	0.32	12.7
HOUR 17	4.3	0.34	12.7
HOUR 18	39.0	3.08	12.7
HOUR 19	80.5	6.43	12.5
HOUR 20	117.6	9.46	12.4
HOUR 21	143.2	11.59	12.4
HOUR 22	130.4	10.58	12.3
HOUR 23	65.9	5.35	12.3
HOUR 24	0.0	.	.
DAY 1	76.3	11.41	6.7
DAY 2	156.9	23.37	6.7
DAY 3	167.6	24.79	6.8
DAY 4	194.4	28.78	6.8
DAY 5	203.1	30.17	6.7
DAY 6	108.6	16.22	6.7
DAY 7	0.0	.	.
LIN	-0.4	-10.79	0.04
COS1	113.9	1.87	6.1
SIN1	-101.0	-18.31	5.5
COS2	20.7	6.69	3.1
SIN2	33.6	8.79	3.8
COS3	11.2	4.28	2.6
SIN3	1.5	0.53	2.7

(continued on the next page.)

Table 9 (Continued). Coefficients of the Fitted Model and Associated Standard Errors and T Values.

Parameter	1000× Coefficient Estimate	T-value	1000× Standard Error
LVIZ	81.6	26.20	3.1
LPRS	70.2	27.82	2.5
LRH	19.2	5.42	3.5
TEM	91.4	18.55	4.9
WDX	58.4	22.28	2.6
WDY	-44.9	-18.67	2.4
RAIN 0	83.4	8.66	9.6
RAIN 1	0.0	.	.
LVIZ*LPRS	-15.9	-7.97	2.0
LVIZ*TEM	40.6	16.07	2.5
LVIZ*WDX	29.9	11.19	2.7
LVIZ*RAIN	61.8	9.75	6.3
LPRS*TEM	-47.2	-20.09	2.3
LPRS*WDX	11.0	5.56	2.0
LPRS*RAIN	-45.8	-8.04	5.7
LRH*TEM	-30.7	-10.17	3.0
LRH*WDY	30.2	12.47	2.4
TEM*TEM	61.1	27.13	2.3
TEM*WDX	37.6	13.15	2.9
TEM*WDY	50.2	16.14	3.1
WDX*WDX	-17.9	-13.75	1.3
WDX*WDY	-30.2	-13.52	2.2
WDY*WDY	-68.0	-41.88	1.6

C The Estimated AR(3) Coefficient Matrices.

For completeness, the estimated AR coefficient \hat{M} matrices of (4) are shown as below:

$100 \times \hat{M}_1$:

1	4	-1	-3	5	-1	4	-3	-1	3	-2	-0	1	1	-0	3	0	-0	-5	6	1	5	9	65
-1	6	-1	-2	5	-6	7	-0	1	-0	-1	0	0	1	2	1	-1	1	-1	3	1	6	8	53
-1	4	-3	1	8	-5	6	-2	0	5	-0	-2	2	3	5	-1	-0	2	-2	1	4	2	12	44
1	6	-4	3	4	-1	5	-2	-3	6	1	-2	4	-0	7	-4	1	0	-1	-1	4	6	8	39
-1	4	-2	-0	7	0	7	-4	-2	7	-0	-2	3	3	2	-4	-2	2	-2	-3	8	7	3	33
-3	3	-4	1	2	7	6	-0	-3	5	1	-1	4	0	0	-1	0	-2	-4	-3	12	3	2	33
0	3	-6	-3	4	1	17	2	-4	3	1	-1	5	1	-1	1	1	-1	-1	-2	4	7	1	24
-5	4	-5	-1	2	1	5	12	1	3	0	-2	1	3	-1	-1	1	2	-1	1	1	1	5	21
-2	-8	-3	6	-2	5	-5	7	7	12	-2	-2	0	2	2	-2	3	2	-3	2	4	3	5	16
-4	-6	-1	0	-1	-2	-1	7	-1	14	6	-1	2	2	1	-0	3	2	-3	0	8	-0	5	13
-4	-1	-1	-2	-3	1	-2	1	-0	13	7	-2	4	2	1	-0	5	-1	-4	1	6	3	4	14
-0	-1	-5	-2	-3	5	-3	4	-3	9	5	2	4	2	4	0	-0	1	-2	2	5	2	7	11
2	2	-8	1	-7	4	2	3	-4	4	4	4	2	5	7	-2	-2	3	-3	3	5	3	8	6
1	2	-6	3	-11	7	2	-1	0	-1	4	1	6	6	4	1	1	3	2	3	3	3	4	5
2	-0	-2	-1	-8	4	2	-1	0	0	4	2	3	3	6	-0	1	3	1	8	4	1	4	2
4	-0	-5	-3	-4	3	-2	1	1	2	-1	5	0	3	2	2	6	3	2	4	8	-2	3	3
4	1	-5	-5	-6	4	-4	3	2	6	-2	0	1	3	6	-2	4	3	7	4	8	-1	3	-0
3	-1	-6	-4	-3	3	-3	2	4	2	-4	5	-3	5	4	-3	1	2	10	10	1	1	2	-1
5	-5	-5	5	-4	0	-6	-0	3	3	-5	4	-1	1	4	-1	0	1	9	11	-2	2	5	2
4	-4	-4	4	-4	2	-4	-2	5	4	-2	1	-4	-0	1	3	1	-5	7	11	5	0	7	0
4	-2	-4	7	-3	4	-5	-2	3	1	-3	4	-6	-2	3	1	3	-7	4	12	4	1	8	3
4	-5	2	2	-0	1	-5	-3	1	1	-0	2	-5	3	2	-0	-1	-1	1	11	1	5	10	1
3	-4	3	3	-1	-1	-2	-2	5	1	1	1	-7	5	4	-1	-4	2	1	12	-1	4	10	1
2	-4	5	2	3	-2	-5	2	2	-0	-2	1	-4	4	7	-4	-0	2	-2	10	1	-1	9	6

$100 \times \hat{M}_2$:

-0	-0	-4	-1	3	2	-4	7	-1	2	-2	-1	1	1	1	1	-2	2	-0	-2	2	-2	-1	-0
-2	3	-3	2	-3	4	-3	7	-2	1	-1	-2	-1	4	-0	1	1	2	-5	2	-1	-1	2	-2
1	3	-0	-2	0	3	-3	8	2	-3	-1	-1	-3	5	-1	4	0	1	-2	0	-4	2	-2	
-1	4	-2	3	-1	5	-6	13	-3	-5	-4	1	-2	5	1	5	-2	0	-4	1	-2	-0	-5	
-3	5	-2	-1	-2	7	-5	16	-2	-4	-3	2	-2	6	2	3	3	-2	-1	-5	4	-1	-6	
1	4	-6	0	-3	11	-2	11	-2	-9	-1	-1	-0	8	0	2	2	-3	-1	-4	5	-5	-3	
-0	3	-4	-2	-3	4	7	9	-2	-7	-1	2	-3	5	5	1	-2	-5	-1	-3	5	-4	-5	
3	3	-4	-4	-1	0	1	17	-6	-6	3	2	-1	3	3	1	-3	-4	-1	-5	3	-0	-0	
5	-0	3	-6	-2	-0	-4	11	0	-4	4	-1	0	-0	3	3	-0	-4	-4	1	-2	4	2	
5	0	6	-11	1	-1	-2	5	1	-2	4	0	-1	2	6	3	1	-4	-4	-0	-1	2	6	
0	2	7	-12	2	-1	0	2	-1	-1	3	2	2	2	1	5	3	-9	-1	-2	-4	7	6	
2	1	9	-8	4	-1	1	-2	5	-7	2	5	2	1	-0	6	2	-9	-3	-0	-3	8	3	
3	-4	7	-8	4	-2	2	-2	3	-4	5	-1	0	6	0	4	3	-6	-2	-2	1	4	5	
-3	4	2	-6	4	-5	-1	1	2	-2	5	-2	1	7	-3	6	0	-1	-2	-7	-1	5	7	
2	3	2	-9	3	-2	-4	2	4	-1	2	3	-6	7	-2	4	1	-2	-0	-2	-3	5	3	
0	2	1	-4	4	-5	0	-2	6	-6	2	2	-2	6	0	3	-1	4	-4	2	-8	7	1	
-3	1	4	-5	5	-6	-2	1	2	1	2	2	0	1	-1	3	-0	4	-3	3	-9	7	-1	
1	-1	4	-4	2	-7	-1	-1	4	3	4	2	-1	2	-5	7	-4	5	1	2	-4	6	4	
-3	-4	7	-10	2	-5	-0	0	5	0	1	-1	-3	3	-3	3	-1	-2	5	3	2	6	3	
-3	-3	1	-7	-3	3	-4	-1	8	2	1	-5	2	1	-4	3	-1	-1	4	4	-1	4	-0	
1	-0	2	-8	-5	4	0	1	8	2	0	-4	2	-1	-3	4	-1	-0	0	1	1	5	0	
-2	7	-3	-8	3	-1	-2	3	9	-0	-1	-5	1	0	-3	5	-1	-0	2	-3	3	3	1	
-2	5	-2	-6	-4	1	2	4	6	-1	-1	-4	3	-3	-2	3	1	-3	1	1	2	-2	2	
-0	7	-2	-9	-2	1	5	2	4	1	-1	-8	2	0	-4	4	3	-7	3	1	-0	1	2	

$100 \times \hat{M}_3$:

2	0	-2	3	-4	1	3	1	-1	-2	2	1	-1	2	-1	1	-0	-1	-2	2	-2	-3	1	4
3	-2	0	3	-2	1	4	2	-2	-4	2	-0	2	-2	1	0	-2	-2	-5	6	-1	-6	4	2
1	2	-3	5	-2	3	2	0	-2	-4	3	-2	3	-2	0	-5	4	-1	-2	2	0	-4	-4	5
2	-1	-6	4	6	1	5	1	2	-8	2	1	0	-2	-1	-4	2	-3	-1	3	-3	-4	-6	4
3	-1	-7	6	3	6	-1	2	1	-10	3	1	1	-1	-1	-3	0	-2	-1	4	-4	-3	-7	5
-2	3	-8	5	2	9	1	4	-1	-8	0	4	-1	0	-3	-1	-2	-4	-2	-0	-1	-2	-5	7
3	2	-9	3	5	4	7	3	-4	-4	0	3	-1	1	-4	-4	-1	-6	4	2	-4	2	-4	6
6	-3	-4	4	5	-1	1	5	3	-5	-2	2	-1	-2	-0	-6	-0	-4	7	4	-3	-0	-3	1
4	0	-5	2	5	-3	-2	3	6	-2	1	4	-1	-6	0	-2	-3	-3	9	1	2	-1	-1	-3
4	1	-6	1	1	-4	-1	1	0	4	6	1	-4	-5	0	-1	-2	1	2	3	-0	-3	3	-5
2	-5	-1	2	4	-6	1	2	1	-2	6	3	0	-5	1	2	-3	-1	4	-3	-2	-1	1	-0
-1	-4	-0	-1	4	-1	1	2	-0	-2	5	2	0	-3	2	-1	-2	-1	2	1	-4	-3	1	-1
0	3	-7	-2	5	-3	6	2	-5	-4	2	-0	2	-2	0	1	-2	-2	2	4	-6	-3	6	1
3	3	-10	-4	4	-0	7	-1	-1	-2	-0	2	-1	-2	4	-3	-1	3	1	2	-4	0	1	2
-1	-1	-3	-4	2	-1	3	2	-5	-1	2	1	-1	-2	5	-3	2	1	5	-5	-0	-0	2	4
-0	-1	-1	-5	2	-0	1	-0	-3	-1	1	2	1	-1	6	-2	2	0	6	-6	-0	2	-4	7
-2	-0	1	-3	2	-4	3	-2	-1	-2	0	4	-1	-2	2	-0	5	-1	7	-3	-6	7	-6	8
-5	2	-3	-1	1	2	-1	-2	2	1	0	3	-7	-1	3	-1	3	-2	10	-3	-8	10	-4	7
-0	2	-3	-4	3	-4	-2	4	5	3	-3	3	-5	1	4	-2	-2	-1	8	1	-6	8	-4	8
2	1	3	-3	-3	-6	4	3	5	-2	0	5	-7	2	-2	-1	-2	1	3	7	-3	8	-7	9
3	-2	0	-3	-2	-4	2	4	1	-0	2	1	-3	2	-3	-2	-2	2	0	4	3	10	-10	4
3	1	-4	-4	-3	-2	1	6	2	-0	1	4	-5	0	-3	-1	3	-2	0	2	4	4	-4	4
2	-3	4	-7	-3	-2	5	5	-1	-1	4	2	-5	1	-2	-0	2	-1	-0	1	0	3	0	4
-1	-1	0	-1	-9	-0	5	5	1	1	0	4	-4	0	-0	-1	-2	4	-5	-0	6	-3	5	3

D The Estimated Kronecker GIW Model.

Recall that for the 10 monitoring sites in the study, the space-time covariance of the Kronecker GIW model (see (5)) is given in terms of $\Lambda \otimes \Omega$. The estimated Λ matrix is:

	Site 1	Site 2	Site 3	Site 4	Site 5	Site 6	Site 7	Site 8	Site 9	Site 10
Site 1	19.74	9.21	14.86	11.28	8.49	13.5	11.43	10.11	11.16	10.42
Site 2	9.21	20.18	10.69	8.79	13.47	11.46	8.81	7.79	9.99	6.67
Site 3	14.86	10.69	24.84	13.61	7.51	17	13.96	11.93	9.49	9.9
Site 4	11.28	8.79	13.61	21.44	8.06	15.32	16.07	15.92	13.46	9.81
Site 5	8.49	13.47	7.51	8.06	26.57	9.46	8.53	8.25	11.6	6.88
Site 6	13.5	11.46	17	15.32	9.46	23.62	16.46	13.04	12.23	10.48
Site 7	11.43	8.81	13.96	16.07	8.53	16.46	22.59	13.83	12.23	8.92
Site 8	10.11	7.79	11.93	15.92	8.25	13.04	13.83	22.65	13.93	12.17
Site 9	11.16	9.99	9.49	13.46	11.6	12.23	12.23	13.93	27.34	14.36
Site 10	10.42	6.67	9.9	9.81	6.88	10.48	8.92	12.17	14.36	27.22

and the estimated Ω matrix ($\times 100$) is:

100	72	69	70	62	54	32	21	15	15	22	22	14	15	12	5	-9	-8	-3	1	10	11	7	4
72	125	102	90	84	72	47	26	19	17	25	26	18	21	23	9	-1	1	4	6	12	13	13	19
69	102	164	139	128	113	76	56	40	38	43	38	26	20	23	15	2	10	-2	-5	4	4	3	14
70	90	139	199	163	147	108	85	66	58	58	52	41	28	23	21	1	5	0	-8	4	7	2	12
62	84	128	163	221	194	144	119	96	87	80	64	50	40	26	28	15	18	8	-1	11	9	5	17
54	72	113	147	194	253	184	146	118	103	96	86	62	46	31	23	12	8	2	-4	12	15	8	21
32	47	76	108	144	184	216	167	130	103	90	80	62	51	34	32	26	23	27	22	29	28	24	27
21	26	56	85	119	146	167	234	180	138	119	96	84	74	59	58	44	45	43	40	39	45	37	36
15	19	40	66	96	118	130	180	234	183	160	128	108	85	71	74	59	60	58	46	43	52	44	49
15	17	38	58	87	103	103	138	183	247	203	169	139	105	88	89	80	79	69	58	46	55	46	56
22	25	43	58	80	96	90	119	160	203	269	223	193	152	119	114	106	91	72	59	53	65	53	65
22	26	38	52	64	86	80	96	128	169	223	290	234	186	154	130	123	107	91	80	79	86	73	83
14	18	26	41	50	62	62	84	108	139	193	234	310	251	206	174	161	144	112	103	93	99	85	90
15	21	20	28	40	46	51	74	85	105	152	186	251	317	250	209	195	168	134	122	102	107	92	94
12	23	23	23	26	31	34	59	71	88	119	154	206	250	315	245	222	192	152	132	118	121	109	117
5	9	15	21	28	23	32	58	74	89	114	130	174	209	245	315	253	214	167	145	123	121	115	113
-9	-1	2	1	15	12	26	44	59	80	106	123	161	195	222	253	317	261	209	181	147	143	137	129
-8	1	10	5	18	8	23	45	60	79	91	107	144	168	192	214	261	320	250	209	171	164	149	138
-3	4	-2	0	8	2	27	43	58	69	72	91	112	134	152	167	209	250	309	246	205	197	178	170
1	6	-5	-8	-1	-4	22	40	46	58	59	80	103	122	132	145	181	209	246	298	243	219	208	193
10	12	4	4	11	12	29	39	43	46	53	79	93	102	118	123	147	171	205	243	288	254	230	217
11	13	4	7	9	15	28	45	52	55	65	86	99	107	121	121	143	164	197	219	254	307	272	256
7	13	3	2	5	8	24	37	44	46	53	73	85	92	109	115	137	149	178	208	230	272	322	289
4	19	14	12	17	21	27	36	49	56	65	83	90	94	117	113	129	138	170	193	217	256	289	335

The estimate of the degrees of freedom of the Inverted Wishart model is $\hat{\delta}^* = 298.6$, implying the estimated degrees of freedom of the marginal matrix-t distribution of $X(d)$ equal to $\hat{\delta} = 298.6 - 10 \times 24 + 1 = 59.6$.